

Charge stability on thin insulators studied by atomic force microscopy

N. Felidj, J. Lambert, C. Guthmann, and M. Saint Jean^aGroupe de Physique des Solides, Universités de Paris 6 et 7^b, Tour 23, 2 place Jussieu, 75251 Paris Cedex 05, France

Received: 19 May 2000 / Revised and Accepted: 22 August 2000

Abstract. Charge diffusion in thin Al_2O_3 layers has been investigated by Atomic Force Microscopy (AFM). The layers were made by anodic oxidation of Al plates, in order to obtain plane and homogeneous amorphous oxides of known thicknesses. Under dry-nitrogen atmosphere, the charges are deposited by contact electrification: a deposit voltage is applied between the Al substrate of the layer and the metallized AFM tip brought to contact with the oxide. This process is perfectly controllable and reproducible, the quantity of charges deposited being proportional to the deposit voltage. Afterwards the tip is lifted up and scans the surface of the oxide in order to observe the diffusion of the deposited charges. Two behaviors were observed for the diffusion process depending on the thickness and on the deposit voltage. These results are interpreted by introducing an inhomogeneous trap distribution in the layer, the diffusion process being considered mainly as diffusion by hopping transport in the bulk.

PACS. 72.20.-i Conductivity phenomena in semiconductors and insulators – 72.20.Ee Mobility edges; hopping transport – 73.20.-r Surface and interface electron states

1 Introduction

Charge transport on insulators is of great interest both scientifically and technologically [1–4]. However, despite its everyday occurrence and a very large experimental investigation with various techniques, this phenomenon remains an unsolved problem. Recently, atomic force microscopy (AFM) was used to scan the electronic transport phenomena in insulators [5,6]. As a local probe, AFM presents some advantages with respect to the macroscopic experiments since it offers the opportunity to reduce the result discrepancies due to the surface and bulk heterogeneities of these materials. Moreover, the diffusion process can be “visualized” directly in contrast with integrated measurements given by macroscopic experiments.

The most recent and complete results obtained on charge diffusion by electrostatic force measurements have been performed on thin silicon oxide [5]. In these experiments, the deposition of electrons by contact of AFM tip on SiO_2 surfaces and their diffusion have been investigated under vacuum and at ambient atmosphere. However their interpretations invoke a quite mysterious “stable-unstable phase transition” of the transferred electrons and no further study has been carried out to determine the parameters controlling this charge diffusion. In order to identify these parameters and in particular to distinguish the different mechanisms involved in charge diffusion (surface

or/and volume diffusion), we have performed new experiments on amorphous alumina surfaces.

In a previous study [6], the electrification by contact or friction of these surfaces had been extensively investigated at submicronic scale using an atomic force microscope in resonant mode; thus the parameters governing the triboelectric effect on these oxide surfaces are well controlled.

In this paper, we report the results concerning the study of the diffusion of charges deposited on alumina layers of various thicknesses ($15 \text{ nm} < d < 100 \text{ nm}$). The characteristic times of diffusion are of about a few hundred seconds and their variations with the initial deposited charge density σ depend on the oxide thickness: for thin oxide layers, a single characteristic time is needed to describe the charge diffusion whereas two time constants are required to describe the diffusion observed for thicker oxide layers.

The samples preparation and characterization are described in Section 2; Section 3 is devoted to the experimental setup and protocols used to deposit and to measure the charges. In Section 4 we present the results concerning the variations of the relaxation times with the thickness of the sample and the initial deposited charge densities. These results will be discussed in Section 5.

2 Elaboration and characterization of alumina samples

Alumina layers grown on Al-plates by anodic oxidation were chosen for these experiments for two reasons: first,

^a e-mail: saintjean@gps.jussieu.fr^b CNRS UA 17

they are good homogeneous insulators; when they are prepared by anodic oxidation, in contrast with thermal oxidation, their surfaces are smooth. In addition their thickness is easy to check during their elaboration. This opportunity is important because we have found in preliminary studies that the thickness of the samples played a role in the charge diffusion process. Secondly previous experiments on these alumina surfaces have shown that a controlled quantity of charges of either positive or negative sign can be deposited; thus the relaxation process of positive and negative carriers can be studied and compared on the same samples [6].

The alumina layers are prepared by anodic oxidation of Al-plates in ammonium pentaborate ($\text{NH}_4\text{B}_5\text{O}_8 \cdot 2\text{H}_2\text{O}$), with constant current (about 1 mA/cm^2) imposed between the Al-plate electrode and a platinum cathode (this current induces the migration of Al^{3+} and O^{2-} ions inside the layers). By measuring the potential bias ΔV inside the oxide, its thickness is determined precisely. In order to calibrate ΔV , we have also evaluated the ^{16}O quantity inside the layer, which is directly proportional to its thickness, by measuring the number of protons produced by nuclear reaction between ^{16}O and deuterons produced in a van de Graaff accelerator [7]. The thicknesses of the samples studied were $d = 15, 30, 60$ and 100 nm .

The samples are transferred afterwards in the vacuum chamber of our experimental setup, which is first out-gassed during 24 h, then filled with dry nitrogen gas to ensure that the oxide surface remains dry. On the other hand, in order to evaluate the influence of contamination on the diffusion processes, other samples of same thicknesses are deliberately left in ambient atmosphere before measurements.

The contamination of the samples left in ambient atmosphere is characterized by X-ray Photoelectron Spectroscopy (XPS) [8]. The XPS signals were recorded using a VG Scientific Scalab MKI system operating in the constant analyzer energy mode. A Mg $K\alpha$ X-ray source was used at a power of 200 W and the by-pass energy was set at 20 eV. The pressure in the analysis chamber was about $5 \times 10^{-8} \text{ mbar}$. The surface composition of various samples was determined by considering the integrated peak areas of Al_{2s} , Al_{2p} , O_{1s} , C_{1s} . Figure 1 exhibits an XPS wide scan obtained on a freshly prepared alumina layer ($d = 15 \text{ nm}$). The scans display peaks due to aluminum and oxygen arising from the alumina layer as well as a peak due to carbon contamination on the oxide surface. The extent of the contamination can be estimated by measuring the relative intensities of the observed peaks. For the $d = 15 \text{ nm}$ samples, the ratio of integrated peak areas $I_{\text{C}}/I_{\text{Al}}$ is 15 times higher for the samples exposed to the ambient atmosphere than for the freshly prepared samples; the same ratios were obtained for the samples of other thicknesses.

We concluded from these measurements that the samples are completely contaminated by various organic molecules when exposed to ambient atmosphere more than a few hours after their making. Thus, only the layers

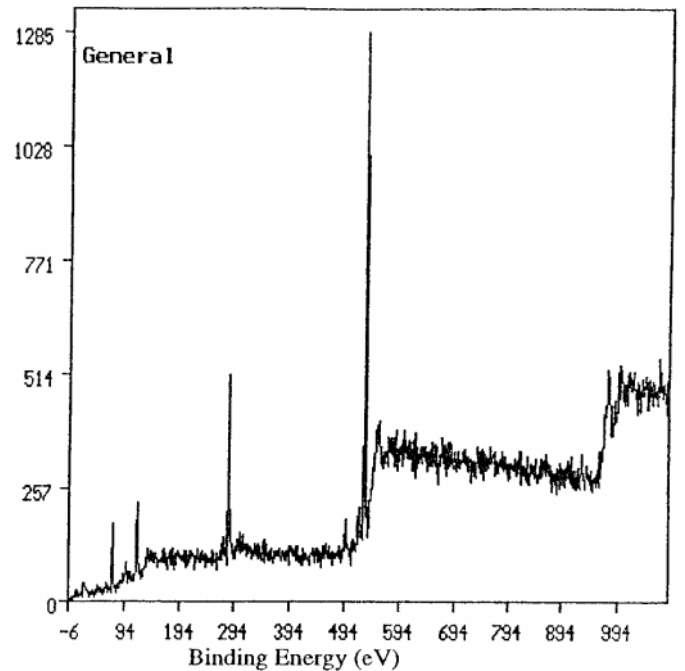


Fig. 1. XPS spectrum of an alumina layer. One can recognize peaks due to aluminum Al_{2s} at 100 eV, Al_{2p} at 75 eV, O_{1s} at 530 eV. The C_{1s} peak at 285 eV is due to carbon contamination on the oxide surface.

transferred in the vacuum chamber in a time less than a few minutes can be considered as “freshly” prepared.

3 Experimental methods and force measurements

We use a homemade Atomic Force Microscope in resonant mode. The tip is made of Si_3N_4 coated with Pt. This metallization allows to deposit and measure charges with the same tip and thus, to avoid any charge loss during the measurements [6]. Moreover the Pt coating presents the advantage of being very stable and of allowing reproducible deposits.

The experimental setup is very similar to the one previously described in [6,9]. The main innovation is the addition of a vacuum chamber containing the sample and the tip, the interferometric detection being outside the vacuum chamber.

The nanometric metallized tip is fixed at the end of a cantilever, the latter being excited at a frequency ω_m selected near its resonance frequency ($\approx 200 \text{ kHz}$). When the tip interacts with an insulator surface fixed or grown on an underlying metallic electrode, the frequency and quality factor of the resonance of the cantilever are modified, which induces a variation of the cantilever vibration amplitude $A(\omega_m)$ measured at ω_m . Moreover, if a voltage $V = V_0 + V_1 \sin \Omega t$ ($\Omega \approx 50 \text{ kHz}$) is applied to the tip, the underlying metallic surface being maintained at zero potential, an additional capacitive force $F(\Omega)$ is exerted on the tip and induces a modulation $A(\Omega)$ of the oscillation

of the cantilever at the frequency Ω . The cantilever vibration is detected by optical heterodyne interferometric detection and analyzed by two lock-in analyzers respectively tuned at the frequencies ω_m and Ω .

From the measurement of the amplitude $A(\Omega)$ we can determine the contact potential V_c associated to the tip-surface system as well as the deposited charge [6,9]. With no deposited charge, $A(\Omega)$ is proportional to $(V_0 + V_c)$; V_c is measured by tuning V_0 until $A(\Omega)$ becomes zero which corresponds to $V_0 = -V_c$. When charges are on the surface, the additional charge-tip force induces a variation of the amplitude $A(\Omega)$ when the tip scans over the charge. By comparing the $A(\Omega)$ measurements before and after contact, the deposited charge can be determined. Simultaneously, the output signal $A(\omega_m)$ is introduced into a feedback loop to control the tip-surface distance. The feedback signal at ω_m is used to image the surface topography; in particular one can verify that its corrugation has not changed after charge deposition.

The charges are deposited by “injection”. The tip stays in contact with the same point of the oxide surface, a “deposit voltage” V_d being applied to the tip: initially far from the oxide, the tip is softly put into contact with the surface by slowly shifting the reference value of the feedback loop. During this down motion, the tip is maintained at $V_0 = 0$ V. When the contact is established, a voltage V_d (-25 V $< V_d < +25$ V) is applied during t_d seconds, then the tip is raised far from the surface, the voltage V_d being in this phase maintained for t_r seconds (1 ms $< t_r < 10$ s) to avoid any charge back flow [11]. We emphasize that the same tip is used for the deposition of charges and for their reading. This requires very strict control of the conditions of experiments. In particular we have verified, performing SEM studies on the tip before and after friction, that the tip and its metallic coating were not damaged during the experiments. In previous experiments, we had shown that no variation of the magnitude of the deposited charge was observed when the times t_d and t_r were tuned between 1 ms and 10 s [6] (in the results presented here, t_d is 100 ms). In addition, we had exhibited the linear variation of the quantity of transferred charges with V_d : $\sigma = 10^{-3} V_d$ C m $^{-2}$.

The tip scans a line of about 1 μ m around the charge deposit during a few minutes. The maximum of amplitude $A_{\max}(\Omega)$ is recorded. It corresponds to the tip being exactly above the deposit, the $A(\Omega) = 0$ reference corresponding to the signal far from the deposit.

Following the procedure proposed by Terris *et al.* [10] and using the method of images to determine the electrostatic force between the tip and the surface, we had previously developed a simple model describing the tip-surface force and had shown that the main contribution to the measured amplitude $A(\Omega)$ is due to the interaction between the deposited charge Q and $q_1 = 4\pi\epsilon_0 R(V_0 + V_c)V_1 \sin \Omega t$ which describes the tip charge due to the applied potential. Neglecting all the other contributions to the force applied to the tip, we can then consider that $A_{\max}(\Omega)$ is proportional to the quantity of deposited charges [6,12].

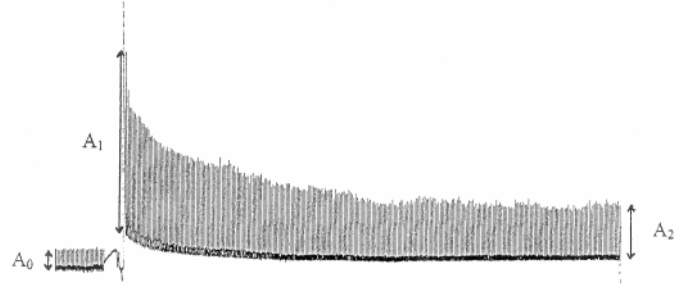


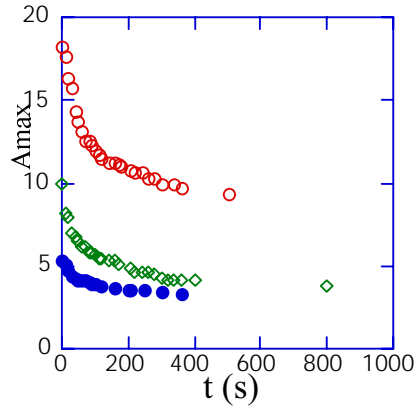
Fig. 2. A typical $A(\Omega)$ versus time variation curve obtained on a thin Al_2O_3 layer. The variation of the amplitude $A_{\max}(\Omega)$ with time is simply the envelop of the curve. The amplitudes A_0 , A_1 and A_2 are represented. The duration of the decrease is approximately 10 mn.

The experiments were performed taking $V_0 = -V_c$ in order to cancel the mean electrostatic field due to the tip in the layer. $A(\Omega)$ and $A(\omega_m)$ are measured simultaneously by using the classical topographic feedback loop procedure in order to be sure the variation of $A(\Omega)$ is not due to a possible mechanical drift of the piezoelectric ceramic.

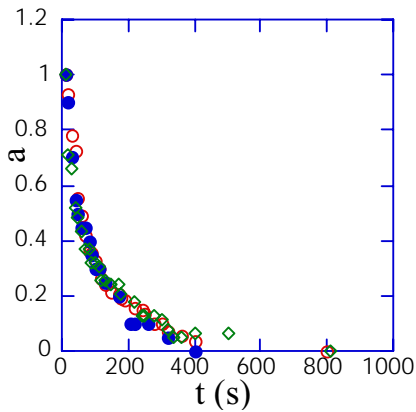
4 Results

Figure 2 presents a typical recorded decrease of $A_{\max}(\Omega)$ with time. Two quantities can be extracted from such a curve: the ratio R of the quantity of charges that have left the oxide after a few minutes with respect to the total quantity of deposited charges, and the time constant τ characterizing the diffusion of the mobile charges. In order to obtain R , we measure three parameters on the recorded curves: the signal amplitudes A_0 just before the contact electrification, A_1 immediately after deposition and A_2 when the signal does not vary anymore, thus R is defined as the ratio $(A_1 - A_2)/(A_1 - A_0)$. The time constants τ describing the relaxation process are determined by fitting the variations of $A_{\max}(\Omega)$ with time decreasing exponentials. In order to compare easily the different results obtained for different samples, the signal amplitude A_0 is subtracted from the amplitude $A_{\max}(\Omega)$ and normalized.

In order to prove that R and τ are relevant to describe the diffusion process, we have checked their reproducibility by comparing their values obtained for similar conditions of deposit. In previous studies, we have shown that the deposition is a reproducible mechanism [6]. Let us now compare the ratio R and the time evolution of charges deposited under the same conditions: Figure 3a shows the amplitude decrease versus time for negative charges deposited in the same conditions at three different points of the same “fresh” alumina surface. The corresponding values of R are identical. In order to compare the different experiments we have defined a normalized amplitude $a = (A_{\max}(\Omega) - A_2)/(A_1 - A_2)$. After normalization (Fig. 3b), the three curves are perfectly superposed. Thus, our recent results allow to consider the diffusion process as reproducible, and confirm that the parameters (R, τ) are



(a)



(b)

Fig. 3. (a) $A_{\max}(\Omega)$ versus time. These three curves are obtained on different spots of the same Al_2O_3 layer using the same deposit conditions ($d = 30$ nm, $V_d = 10$ V). The Y-axis scale is graduated in arbitrary units; (b) here is represented the normalized variation of $A_{\max}(\Omega)$, *i.e.* $a = (A_{\max}(\Omega) - A_2)/(A_1 - A_2)$. After normalization, the three curves are superimposable.

relevant to characterize the diffusion processes and can be used to compare the results obtained for different samples.

First, let us present the results obtained for freshly prepared samples of different thicknesses ($d = 15, 30, 60$ and 100 nm). On each layer, different quantities of charges were deposited. These experiments were carried out under dry- N_2 atmosphere.

The first important result is that the quantity of charges stored on/in the oxide a long time after the deposit depends on the sample thickness. The ratio R for sample thicknesses larger than 15 nm is systematically smaller than 1 whatever the initial charge quantity is, indicating that the deposited charges have not completely diffused and that some of them are stored in the oxide layer, trapped on surface or bulk sites. In

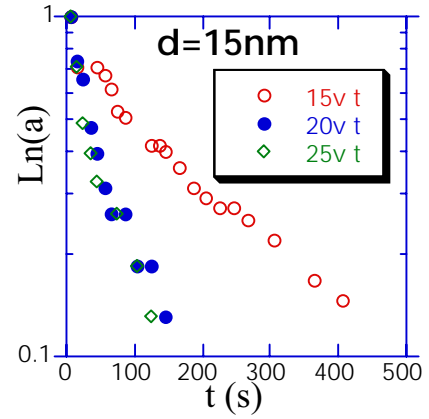


Fig. 4. Normalized amplitude variation in logarithmic scale. On a fresh 15 nm thick Al_2O_3 layer, the charge diffusion has only one characteristic time, depending on the deposit voltage, here 15 V, 20 V and 25 V.

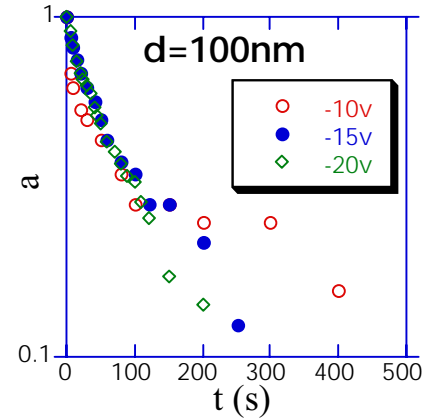


Fig. 5. Normalized amplitude variation in logarithmic scale. On a fresh 100 nm thick Al_2O_3 layer, the charge diffusion has two characteristic times depending on the deposit voltages, here -10 V, -15 V and -20 V.

contrast, this ratio is equal to 1 for the thinnest samples ($d = 15$ nm). This means that all the charges have disappeared. The crossover thickness for storage capacity being about 30 nm.

Another thickness-dependent behavior is the variation of $A_{\max}(\Omega)$ with time. For the thinnest samples, the decay of $A_{\max}(\Omega)$ can be described with only one characteristic time whereas for the thickest samples, two times are required to describe the evolution of the force applied to the tip. As for the R ratio, the crossover seems to occur for a thickness about 30 nm. For instance, Figure 4 presents the recorded decrease of $A_{\max}(\Omega)$ when negative charges are deposited on 15 nm samples, with various deposit voltages V_d . Whatever the deposit voltage is, the dependence of $\text{Ln}(A_{\max}(\Omega))$ with time is roughly linear, thus indicating that, in this case, the diffusion process can be described by only one time constant. In contrast, the measurements obtained for a $d = 100$ nm sample clearly exhibit two characteristic times as shown in Figure 5. For the three injection voltages, $A_{\max}(\Omega)$ decays at first with

Table 1. Thickness $d = 15$ nm.

Deposit voltage V_d	Characteristic time τ
-20 V	80 s
+10 V	250 s
+20 V	150 s
+25 V	120 s

Table 2. Thickness $d = 100$ nm.

Deposit voltage V_d	Characteristic times τ_1 and τ_2	
-10 V	100 s	400 s
-15 V	100 s	200 s
-20 V	100 s	100 s

a characteristic time of about 100 s followed by a slower process characterized by a second time constant (Tab. 2). The same behavior is observed with a 60 nm thick layer, the first time being in this case about 50 s.

We have studied the variations of these characteristic times with the potential V_d which is proportional to the number of charges initially deposited [6]. For $d = 15$ nm samples, the only relaxation time τ observed decreases with the amplitude of the deposit voltage (see Tab. 1). For thicker samples, the first time constant τ_1 is independent of the deposit voltage, whereas the second long relaxation time τ_2 is voltage-dependent, as for thin samples. The higher the voltage is, the faster the amplitude decreases (see Tab. 2). The variations of the time constants with V_d are similar for both polarities, however smaller times are measured for negative V_d .

At last, in order to evaluate the influence of the surface contamination on the diffusion process, negative and positive charges were deposited on surfaces which had been left a few days in ambient atmosphere. The observed time evolutions are radically different from those observed for “freshly” prepared samples kept in dry nitrogen gas. The first point is that, whatever the oxide thickness or the deposit voltage are, all the measured ratios R are equal to 1. This result indicates first that the totality of the deposited charges systematically disappears when oxide surfaces have been exposed to ambient atmosphere. Charges can be deposited but not stored in this type of samples. The second point concerns the time dependence of $A_{\max}(\Omega)$. For two deposit voltages ($V_d = 15$ V and 20 V), the charge diffusion on a sample of thickness 15 nm can be described by only one characteristic time. The relaxation of charges deposited on 100 nm samples for similar V_d potentials can also be described by a single time constant. This time, as for thin samples, is about 200 s and is independent of the deposit voltage. The likeness of these behaviors suggests that the diffusion of charges for these polluted samples occurs exclusively on the surface of the insulator and is probably due to the contaminants or to the water film present on the surface.

5 Discussion

From now on, we shall only discuss the results obtained on fresh samples. Different conduction mechanisms can be invoked in insulating materials with traps. Some of them involve the conduction band whereas others only consider the hopping conduction between traps [13–18]. The predominance of either phenomenon depends on the strength of the electric field in the layer and on the temperature. In amorphous materials like alumina, the high resistivity is generally attributed to localized states in the forbidden band [17, 18]. Moreover, our previous results [6] indicated that the traps played a central role in the electrification of these oxides: the charges are transferred on trap levels, the large concentration of trapped charges inducing the pinning of the chemical electropotential in the surface insulator. This indicates that the mechanism of the carrier transport through these oxides is certainly controlled by hopping process, the large values of the observed time constants confirming this assumption [19].

Once the tip is retracted, the charge transport is dominated by the conduction induced by the electric field in the bulk of the insulator. The electric field is produced by the deposited charges and by their images in the Al-substrate. One could argue that the tip contributes to the charge displacement *via* the $V_0 + V_1 \sin \Omega t$ voltage applied between the tip and the aluminum electrode. Actually three reasons make this contribution negligible: firstly, the V_0 voltage is chosen to be equal to $-V_c$ so that there is no continuous voltage between the bulk of the insulator and the tip. Secondly, the frequency Ω of the alternative voltage V_1 is 50 kHz, which is much too high when compared to the characteristic times observed experimentally ($\langle V_1 \sin \Omega t \rangle \tau = 0$), and thirdly because the tip sweeps a large area compared to the charge extension and is most of the time too far from the charges to influence them.

In this scheme our interpretation is based on the fact that the hopping characteristic time depends on the barrier height between the traps, which is modified by the electric field in the oxide, and on the inter-trap distance [13, 18]. Since we observe two characteristic times in the charge spreading, the main assumption to interpret our results is to consider the oxide layers as inhomogeneous with respect to the trap distribution. Let us point out that, since the inter-trap distance dependence of the hopping characteristic time is exponential, this inhomogeneity is not necessarily very large: for instance, the characteristic time can vary from 26 s for a 30 Å trap distance to 12.5 min for a 33 Å trap distance [18, 20]. This assumption is justified by several experimental results. The very fast and important charge transfer observed in previous triboelectricity experiments suggested a quasi-equilibrium between the tip and a region under the surface with a large concentration of traps, the characteristic penetration length being about 50 nm [6]. The change in the time behavior of the amplitude (crossover between one characteristic time and two characteristic times) observed in the present experiments when the oxide layer thickness is about 30 nm confirms the order of magnitude of this penetration length. Hence we assumed here that the trap

distribution is very large at distances from the surface less than 30 nm and weaker for larger distances. This assumption is in agreement with the literature comments on electronic levels in oxide surfaces which mention trap concentrations differing by a few orders of magnitude between the surface and the bulk [18,21].

Under this assumption, thin oxides ($d < 30$ nm) present only one large concentration of traps. Since these traps are “instantaneously” filled during the injection, the hopping time between them is very short with respect to the measured time constants. Once the tip is removed, all the charges located in the insulator bulk migrate under the force exerted by their images to the traps that are the nearest to the Al_2O_3 -Al interface. The characteristic time of this migration is similar to the injection one, since the hopping process involved is the same. Therefore this migration will be considered as instantaneous as well. Then, the charges trapped near the Al_2O_3 -Al interface, being assisted by the electric field, begin to jump in the conductor. In this case, the observed decrease of the amplitude is due to charges passing from the insulator to the metallic Al electrode and is therefore characterized by only one time constant τ . The other main observation concerning this characteristic time is its deposit voltage dependence. The results obtained can be explained by the fact that the electric field being proportional to the deposited charge density, the barrier-height of the Al_2O_3 -Al interface is lowered when V_d increases. So, the higher the initial charge concentration, the smaller is the diffusion time. The third point about the measures performed on thin layers is the value of the ratio R . It is found systematically equal to 1, so that one could assume that the totality of the deposited charges leave the insulator. Yet, some residual charges could remain trapped since, during this oxide discharge, the local electric field is decreasing; this decrease would cause the characteristic time to increase beyond the recording duration. Nevertheless this increase should occur for very low concentrations of charges since $R = 1$.

The situation is very different for thicker layers: one can distinguish two regions corresponding to two different trap concentrations. The “surface region” (at distances smaller than about 30 nm from the surface) presents a higher concentration of traps than the “bulk region” (at distances higher than about 30 nm from the surface). During the injection, only the “surface region” traps are filled instantaneously. Once the tip is retracted, these trapped carriers are attracted by their image charges. The carriers trapped in the “surface region” first cross the “bulk region” and, once they are located in the nearest Al electrode traps, jump in the metal. This process permits to explain the two-times behavior of the amplitude decrease: the first characteristic time is associated to the migration of the charges across the “bulk region” whereas the second one is related to the Al_2O_3 -Al interface crossing.

The most obvious argument in favor of this interpretation is the similarity observed between the time constants τ measured for thin layers and τ_2 measured for thicker ones; their variations with the deposit potential

suggest that they describe the same relaxation process. Once τ_2 and τ are considered to be alike, the fact that this time is independent of the oxide thickness is a supplementary argument in favor of the localized character (here the Al_2O_3 -Al interface) of the process it is related to. The second point is that the first time τ_1 , which is likely to describe the “bulk region” crossing, increases with the oxide thickness. It is found to be independent of the initial transferred charge (or deposition potential V_d); indeed the electric field is small and the characteristic time between two jumps is roughly proportional to the exponential of the distance between traps (the concentration of trap being small).

The migration across the “bulk region” permits to explain why the measured values of the ratio R are systematically inferior to 1 for thick oxides. During the migration process some charges are kept by traps as the electric field becomes too weak to ease their migration.

6 Conclusion

Our studies of the diffusion of charges deposited on thin alumina layers using an AFM in resonant mode led us to a better understanding of the phenomena involved in the charge diffusion in alumina layers. First, the ability for charge storing depends on the layer thickness. The thicker the layer, the larger is the quantity of charges retained. No charge can be stored on samples thinner than 30 nm. Secondly, the time dependence of the diffusion process is also strongly dependent on the layer thickness. Whatever the layer thickness is, the storage and the diffusion are interpreted using charge trapping/detrapping mechanisms. Two successive processes are proposed to explain the observed behaviors: the transport of charges across the bulk and their passing through in the Al electrode. In a previous article we had discussed the charge diffusion during the contact electrification [6]. The results presented here show that, except for the contaminated layers, the surface diffusion mechanism can be neglected, the dominant diffusion occurring in the bulk.

Beyond these results related to alumina oxides, these experiments show that the AFM microscopy is a promising technique to study the charge transport processes in insulators.

References

1. J. Lowell, A.C. Rose-Innes, *Adv. Phys.* **29**, 943 (1980).
2. A.A. Rychkov, G.H. Cross, M.G. Gonchar, *J. Phys. D. Appl. Phys.* **25**, 986 (1992).
3. C. Noguéra, *Physique et Chimie des surfaces d'oxyde* (Ed. Eyrolles and CEA, 1995).
4. D.A. Hays, *J. Chem. Phys.* **61**, 1455 (1974).
5. S. Morita, T. Uchihashi, T. Okusako, Y. Yamanishi, T. Oasa, Y. Sugarawa, *Jpn. J. Appl. Phys.* **35**, 5811 (1996) and references therein.
6. M. Saint Jean, S. Hudlet, C. Guthmann, J. Berger, *Eur. Phys. J. B* **12**, 471 (1999).

7. J. Siejka, J.P. Nadai, G. Amsel, J. Electrochem. Soc. **118**, 727 (1971).
8. J.F. Watts, Vacuum **45**, 653 (1994).
9. S. Hudlet, M. Saint Jean, D. Royer, J. Berger, C. Guthmann, Rev. Sci. Instrum. **66**, 2848 (1995).
10. B.D. Terris, J.E. Stern, D. Rugar, H.J. Mamin, Phys. Rev. Lett. **63**, 2669 (1989).
11. J. Lowell, J. Phys. D Appl. Phys. **12**, 1541 (1974).
12. M. Saint Jean, C. Guthmann (to be published).
13. P. Hesto, *Instabilities in silicon devices*, edited by G. Barbottin, A. Vapaille (Elsevier Science Publishers B.V., North Holland, 1986), p. 263.
14. A.I. Rudenko, V.I. Arkhipov, Philos. Mag. B **45**, 177 (1982).
15. V.I. Arkhipov, A.I. Rudenko, Philos. Mag. B **45**, 189 (1982).
16. A.I. Rudenko, V.I. Arkhipov, Philos. Mag. B **45**, 209 (1982).
17. H. Krause, Phy. Stat. Sol. A **52**, 565 (1979).
18. H. Krause, Phy. Stat. Sol. A **36**, 705 (1976).
19. N. Cusack, *The Electrical and Magnetic Properties of Solids* (Ed. Longmans, 1958), p. 230.
20. I. Lundström, Ch. Svensson, J. Appl. Phys. **43**, 5045 (1972).
21. W.J. Brennan, J. Lowell, M.C. O'Neill, M.P.W. Wilson, J. Phys. D Appl. Phys. **25**, 1513 (1992).